

Five years of optical and infrared monitoring of Betelgeuse with the Himawari-8 meteorological satellite

Daisuke Taniguchi, Kazuya Yamazaki, and Shinsuke Uno (The University of Tokyo)

Based on Taniguchi et al. 2022 (*Nature Astronomy*, 6, 930)

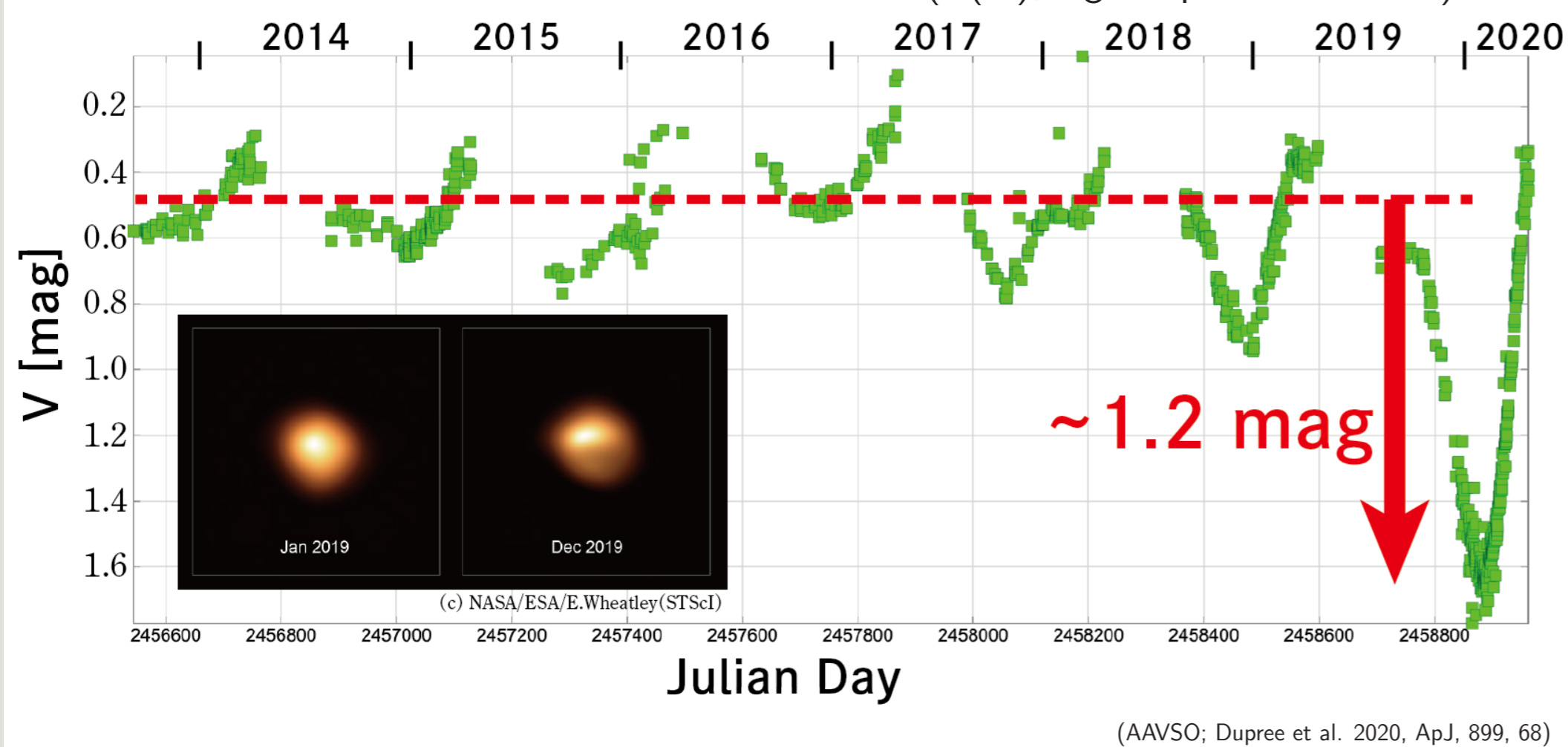
1. Abstract—The Great Dimming of Betelgeuse

Red supergiants are a class of massive stars, who will soon end their lives as supernovae. Time variability at this stage, such as pulsation and mass loss, gives close insights into several fields including massive star evolution and supernova light curves. As a laboratory of the time variability of red supergiants, we focus on the Great Dimming of Betelgeuse in early 2020, an unusual fall and rise in the optical brightness by ~ 1.2 mag. Here we present 16-bands photometry of Betelgeuse in $0.45\text{--}13.5\mu\text{m}$ from January 2017 to today making use of the images taken by the Himawari-8 meteorological satellite. Analyzing these light curves, we show that two mechanisms, a decreased effective temperature and an enhanced dust extinction, may have both contributed to the Great Dimming by the same amounts. We also discuss the future ability of meteorological satellites for the time-domain investigation of other evolved stars.

Data available at: https://d-taniguchi-astro.github.io/homepage/Data_Himawari_en.html

2. Introduction—The Great Dimming of Betelgeuse

- Fainting in the optical in late 2019–early 2020 (Montargès et al. 2021).
- Historical minimum; decreased by $\Delta V \sim 1.2$ mag.
- Scenario 1: Decreased effective temperature (T_{eff} ; e.g. Harper et al. 2020).
- Scenario 2: Increased circumstellar-dust extinction ($A(V)$; e.g. Dupree et al. 2020).



4. Results: the cause of the Dimming

From optical-NIR data:

- The Great Dimming (1.2 mag) was due to
 - Decreased T_{eff} (0.6 mag)
 - Increased $A(V)$ (0.6 mag)
- Dust condensation might have started 8 months before the Dimming?
- BUT, this result is affected, a lot, by the model uncertainty.

From MIR data:

- Thanks to mid-infrared bands ($9.64, 10.41, 11.24\mu\text{m}$), we can trace the time-variable strength of the silicate-dust emission.
- We found that the silicate τ_{10} was enhanced during the Great Dimming, which demonstrates the enhanced dust formation during the Dimming.

From $6\mu\text{m}$ light curve:

- In early April 2019,
 - T_{eff} decreased and stopped.
 - $A(V)$ started increasing.
 - H_2O band underwent a rapid transition from an absorption to an emission.

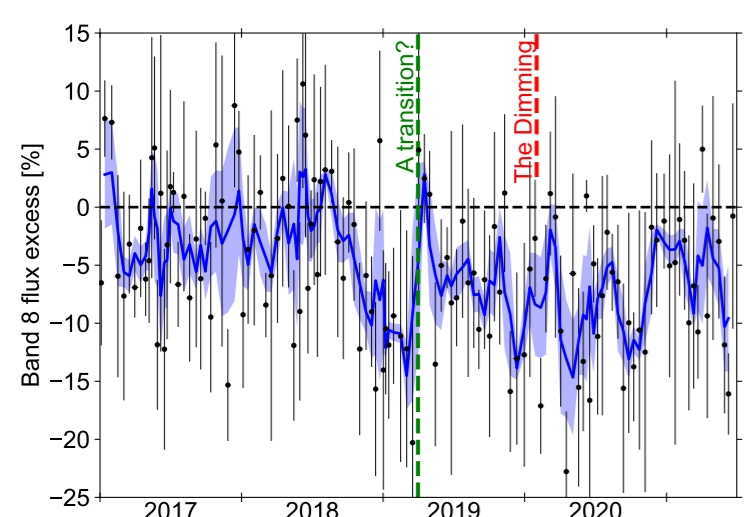


Figure 1: Flux excess in $6\mu\text{m}$, which might be attributed to the H_2O absorption or emission (negative or positive values, respectively).

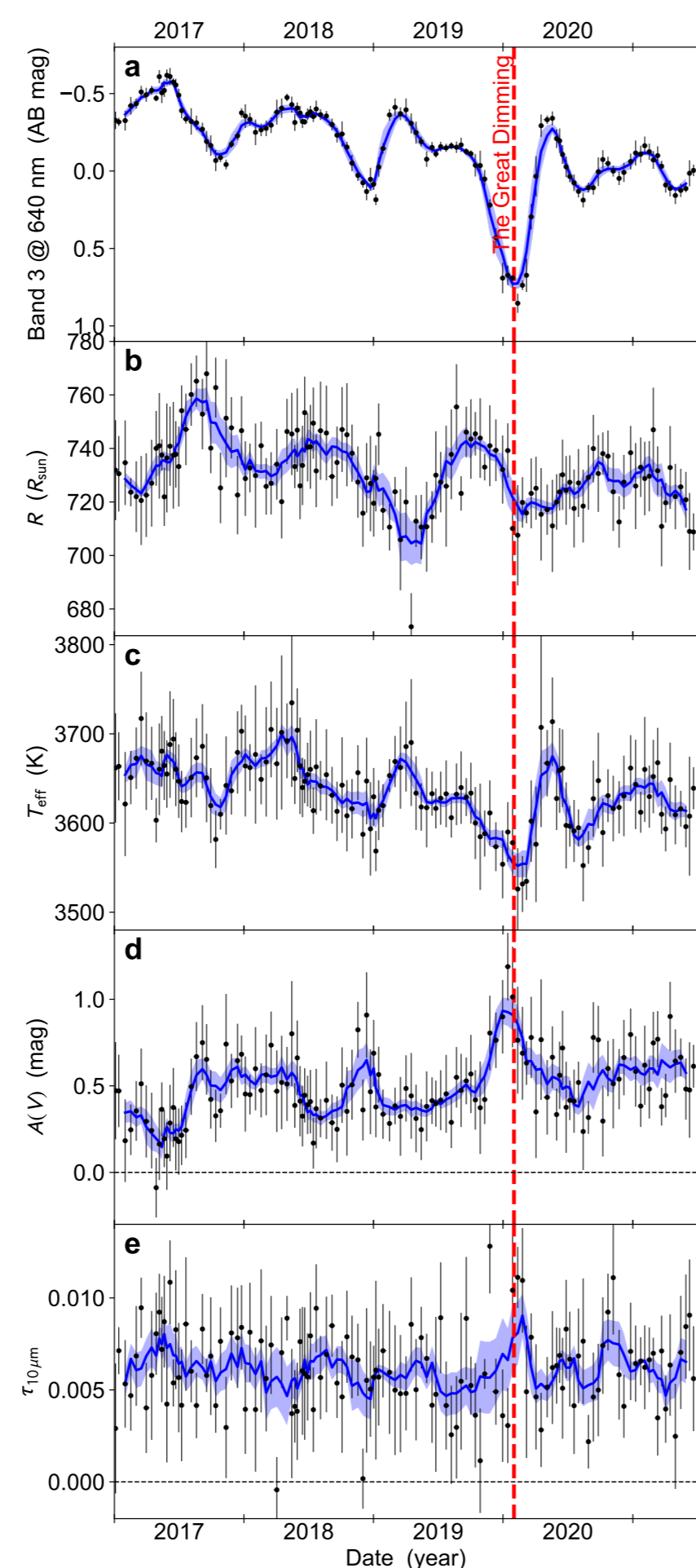


Figure 2: Resultant time-series of the stellar parameters of Betelgeuse.

3. Observed data: Himawari-8 meteorological satellite

- Himawari-8 is a Japanese geostationary meteorological satellite, which is used for daily weather forecasting in Japan (Bessho et al. 2016).
- We found a “pale red dot”, by zooming up the top right corner of the image of the Earth’s disk.

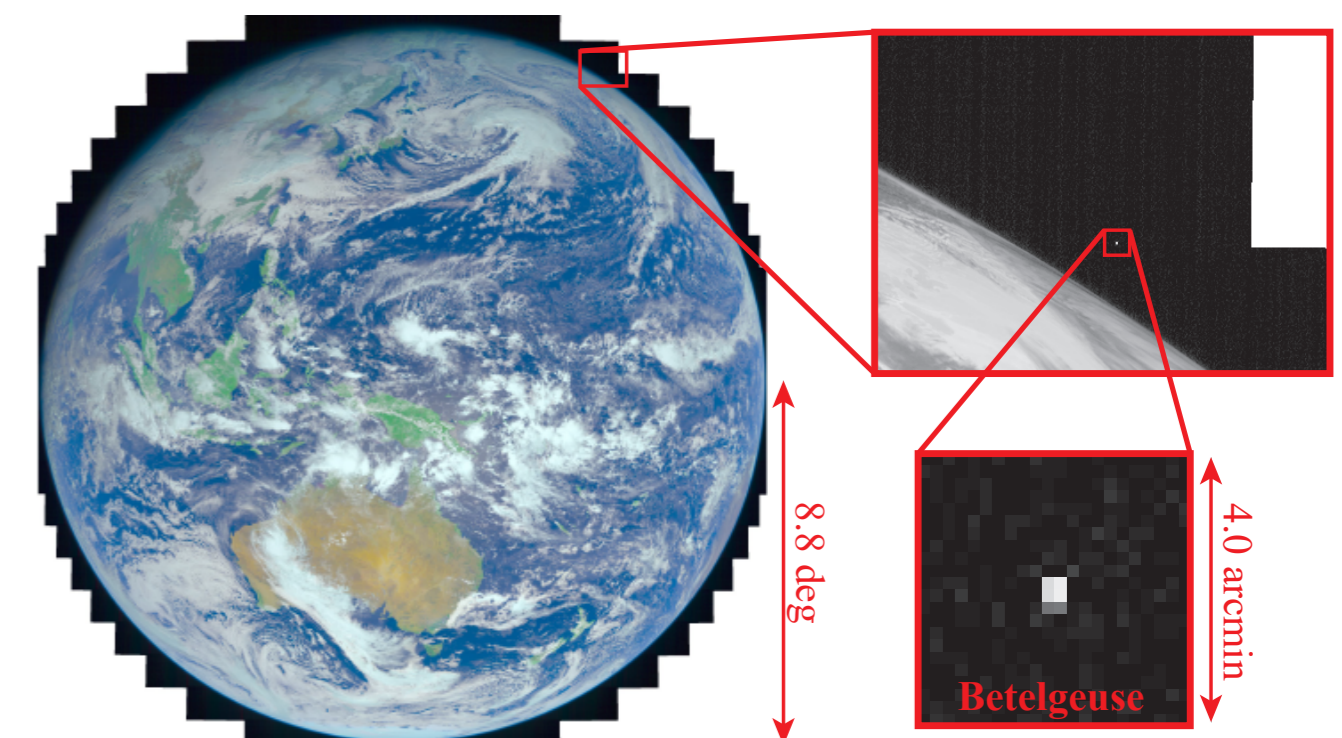


Figure 3: The image of the Earth’s disk taken by the Himawari-8 meteorological satellite on 19 January 2020.

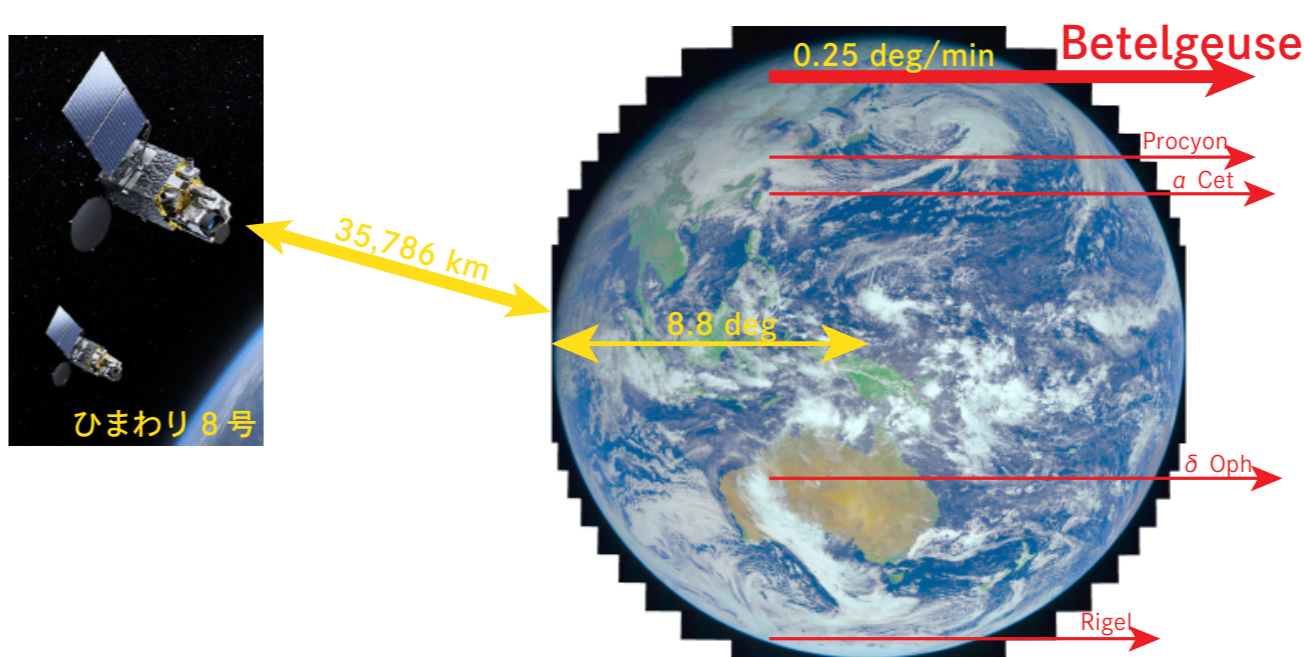


Figure 4: The bright stars that we have observed with Himawari-8.

- Extremely bright stars with $-8.8 < \text{Dec} < +8.8$, every day.
- Early-type stars: Rigel (B supergiant), Procyon (F dwarf)
- Late-type stars: alf Cet, del Oph (KM giant), Betelgeuse (red supergiant)

- 16 bands between optical and mid infrared.
- Advantage to observation in the mid infrared for dust and H_2O .

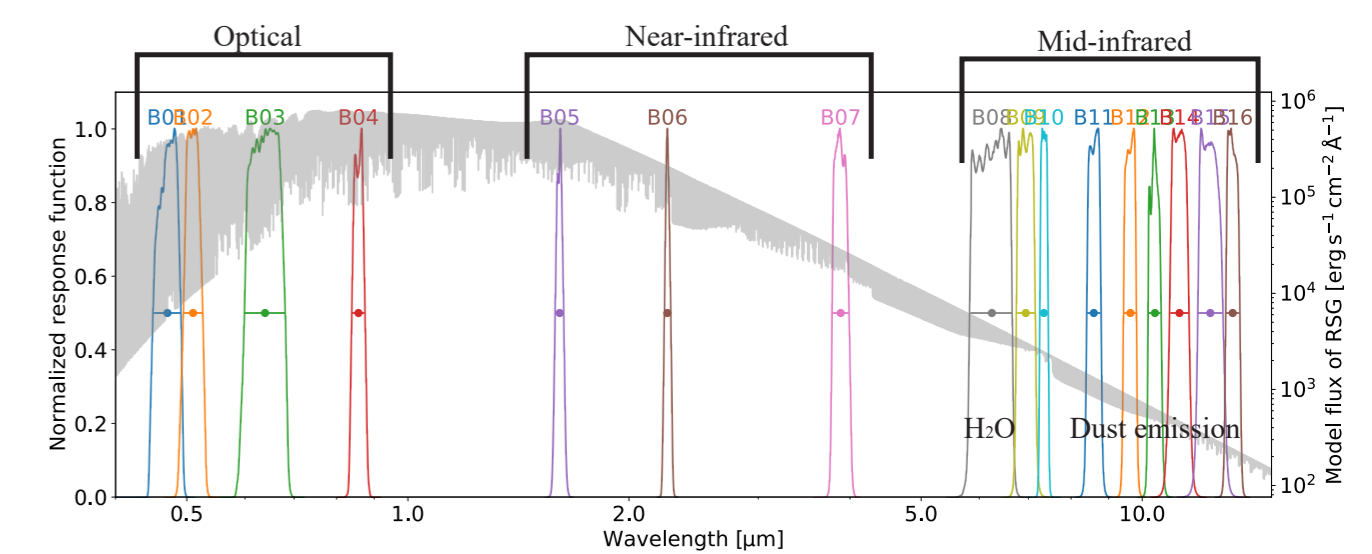


Figure 5: The wavelength coverage of Himawari-8.

Table 1. Basic property of Himawari-8 AHI’s image.

Band No.	λ_0^a (μm)	$\Delta\lambda^a$ (μm)	Pixel scale (km)	Pixel scale (arcsec)	m_{AB}^c (mag)	F_{max}^d ($\text{nW m}^{-2} \mu\text{m}^{-1}$)
(1)	(2)	(3)	(4)	(5)	(6)	(7)
1	0.471	0.041	1.0	5.76	2.4	597
2	0.510	0.031	1.0	5.76	2.5	560
3	0.639	0.082	0.5	2.88	2.4	121
4	0.857	0.034	1.0	5.76	0.8	288
5	1.610	0.041	2.0	11.53	0.7	287
6	2.257	0.044	2.0	11.53	0.9	89.1
7	3.89	0.20	2.0	11.53	2.0	40.2
8	6.24	0.82	2.0	11.53	0.3	29.9
9	6.94	0.40	2.0	11.53	-0.1	36.4
10	7.35	0.19	2.0	11.53	-0.3	38.8
11	8.59	0.37	2.0	11.53	-0.7	50.6
12	9.64	0.38	2.0	11.53	-0.8	49.7
13	10.41	0.42	2.0	11.53	-1.2	47.5
14	11.24	0.67	2.0	11.53	-1.0	44.3
15	12.38	0.97	2.0	11.53	-1.4	39.4
16	13.28	0.56	2.0	11.53	-2.5	36.0

^aEach band is centered on λ_0 with the FWHM of $\Delta\lambda$; see the response function via https://www.data.jma.go.jp/mscweb/en/himawari89/space_segmet/spsg_ahi.html.

^bSpatial resolution at the sub-satellite point, namely 35,786 km from the satellite.

^cSky- 3σ limiting AB magnitude of each band.

^dMaximum valid flux per pixel in the calibrated L1B dataset.

Conditions of detectable stars:

- $|\text{Dec}|$ between $\sim 1\text{--}8.8$ deg
- One of the following:
 - Brighter than 3σ limiting magnitudes in two bands.
 - Extremely bright in one band.

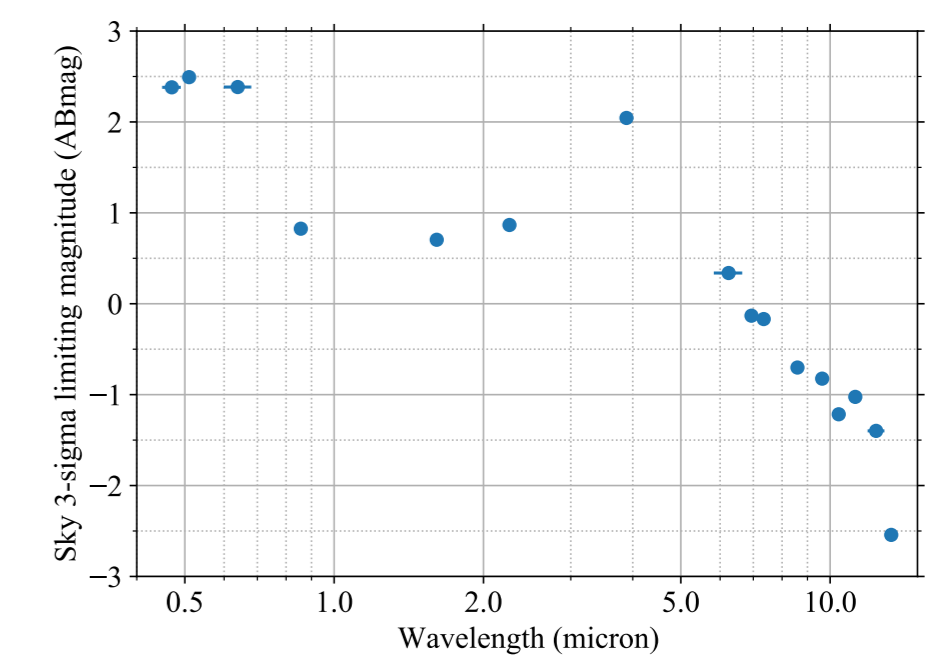


Figure 6: Limiting magnitudes of the Himawari-8 observation.

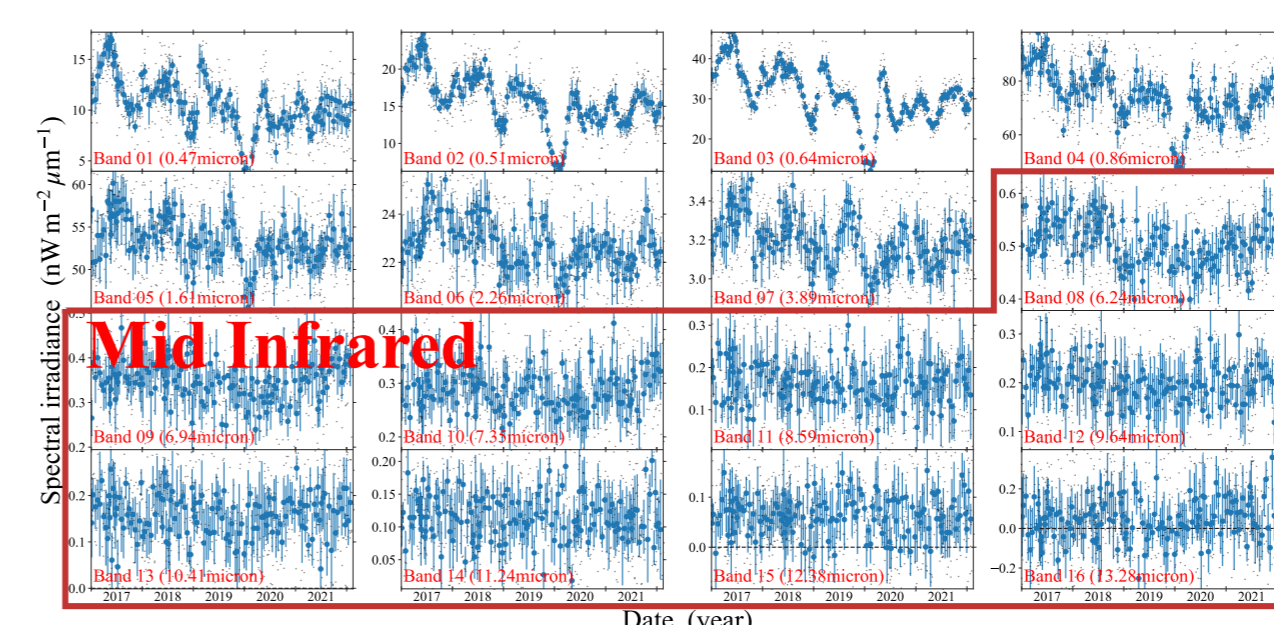


Figure 7: Observed light curves of Betelgeuse.

- Example: 4.5-year light curve of Betelgeuse
- Typically, once per 1.8 days, un-interrupted by the Sun!
- Optical, near infrared, and even mid infrared!

References

- Taniguchi, D., et al. 2022, *Nature Astronomy*, 6, 930
- Montargès, M., et al. 2021, *Nature*, 594, 365
- Harper, G. M., et al. 2020, *ApJ*, 905, 34
- Dupree, A. K., et al. 2020, *ApJ*, 899, 688
- Bessho, K., et al. 2016, *JMeSJ*, 94, 151